Identification of Protein Radicals Formed in the Human Neuroglobin−H_2O_2 Reaction Using Immuno-Spin Trapping and Mass Spectrometry[†]

Olivier M. Lardinois,*[,‡] Kenneth B. Tomer,[§] Ronald P. Mason,[‡] and Leesa J. Deterding[§]

Laboratory of Pharmacology and Laboratory of Structural Biology, National Institute of Environmental Health Sciences, Research Triangle Park, North Carolina 27709

Received April 30, 2008; Revised Manuscript Received July 25, 2008

ABSTRACT: Neuroglobin (Ngb) is a recently discovered protein that shows only minor sequence similarity with myoglobin and hemoglobin but conforms to the typical 3-over-3 α-helical fold characteristic of vertebrate globins. An intriguing feature of Ngb is its heme hexacoordination in the absence of external ligands, observed both in the ferrous and in the ferric (met) forms. In Ngb, the imidazole of a histidine residue (His-64) in the distal position, above the heme plane, provides the sixth coordination bond. In this work, a valine residue was introduced at position 64 (H64V variant) to clarify the possible role(s) of the distal residue in protecting the heme iron of Ngb from attack by strong oxidants. SDS−PAGE analyses revealed that the oxidation of the H64V variant of metNgb by H_2O_2 resulted in the formation of dimeric and trimeric products in contrast to the native protein. Dityrosine cross-links were shown by their fluorescence to be present in the oligomeric products. When the spin trap 5,5-dimethyl-1-pyrroline *N*-oxide (DMPO) was included in the reaction mixture, nitrone adducts were detected by immuno-spin trapping. The specific location of the DMPO adducts on the H64V variant protein was determined by a mass spectrometry method that combines off-line immuno-spin trapping and chromatographic procedures. This method revealed Tyr-88 to be the site of modification by DMPO. The presence of His-64 in the wild-type protein results in the nearly complete loss of detectable radical adducts. Together, the data support the argument that wild-type Ngb is protected from attack by H_2O_2 by the coordinated distal His.

Neuroglobin (Ngb)[1] is a recently discovered protein that belongs to the globin family of proteins (*1*). Like other globins, Ngb reversibly binds small ligands such as dioxygen (O_2), nitric oxide (NO), and carbon monoxide (CO) via an iron (Fe^{2+}) ion of the heme group (*2, 3*). Comparison of Ngb amino acid sequences with those of other vertebrate globins such as myoglobins (Mb) and hemoglobins (Hb) shows only a minor degree of similarity (<21 and <25% identity, respectively) (*1, 4*). Nevertheless, X-ray crystallographic studies performed on both human and murine Ngbs clearly indicate that the two proteins conform to the canonical 3-over-3 α-helical fold characteristic of vertebrate globins (*5, 6*). Ngb was initially discovered in the human and murine brains, and since then, it has been identified in a wide range of vertebrate species (*1, 7*−*11*). In the rat, Ngb is expressed in the cerebral cortex, hippocampus, thalamus, hypothalamus, and cerebellum of the brain (*9, 12*). Ngb is also found in nonneural cells of the endocrine system such as the pituitary gland, the adrenal gland, and the testis (*1, 10*).

A distinguishing characteristic of Ngb is its heme hexacoordination in the absence of external ligands, observed both in the ferrous and in the ferric (Fe^{3+}, met) forms (*2, 5, 6*). This contrasts with the heme environment of Hb and Mb, showing pentacoordination in the ferrous form and distal water coordination for the ferric form of the protein. In Ngb, the imidazole of a histidine residue (His-64) provides the sixth coordination bond, which needs to dissociate thermally from the heme iron before an external ligand can bind. Rapid mixing and flash photolysis experiments have demonstrated that the overall affinity constant for O_2 or other exogenous ligands results from a competition with the internal ligand, the His-64 residue (*2, 3, 13*). Therefore, ligand affinity is not modulated exclusively by the on and off rate constants for the pentacoordinate state.

An additional unusual feature of Ngb that distinguishes this protein from Mb and Hb is the presence of a wide internal cavity [∼120 Å^3 for human Ngb (*5*)] enclosing part of the heme distal site. This peculiarity was first observed in three-dimensional (3D) structures of human and murine Ngb in their ferric form (*5, 6*). Later, the determination of the murine Ngb structure in the CO-ligated state (*14*) revealed an unprecedented heme sliding mechanism for binding the CO ligand. In this mechanism, His-64 essentially retains its position, but the docking of the heme in a new position, deeper inside the internal cavity, creates enough space at the sixth heme coordination site to accommodate the external ligand.

[†] This work has been supported by the Intramural Research Program of the National Institutes of Health and the National Institute of Environmental Health Sciences.

* To whom correspondence should be addressed. Telephone: (919) 541-0341. Fax: (919) 541-1043. E-mail: lardinois.olivier@gmail.com.

[‡] Laboratory of Pharmacology.

[§] Laboratory of Structural Biology.

[1] Abbreviations: DMPO, 5,5-dimethyl-1-pyrroline *N*-oxide; ELISA, enzyme-linked immunosorbent assay; ESI, electrospray ionization; Ngb, neuroglobin; metNgb, metneuroglobin.

10.1021/bi800771k CCC: $40.75
Published on Web 09/04/2008

In addition to this heme sliding mechanism, another component of Ngb that may also affect its ability to bind exogenous ligands is the oxidation state of two reactive thiols (Cys-46 and Cys-55, in human Ngb). Formation of an intramolecular disulfide bond between these two cysteine residues increases O_2 affinity up to 10-fold, presumably by making the heme pocket more accessible to the solvent (*15*). However, the general physiological relevance of this observation is questionable because Cys-46 is absent in other mammalian Ngbs (*16*).

The general physiological functions of pentacoordinated vertebrate globins are well-defined. In humans and other vertebrates, Hb is localized to erythrocytes and transports O_2 between the lungs and other tissues (*17*). Mb, typically found in skeletal and cardiac myocytes, facilitates O_2 diffusion or acts as an NO oxygenase, converting potentially toxic NO to the innocuous nitrate (*18*). However, the precise physiological functions of Ngb and most other newly discovered hexacoordinated globins are, as yet, unclear. It seems unlikely that Ngb functions as an oxygen storage or delivery protein in the brain because of its fairly low concentration in the neurons (~1 μM) (*1*) and its weak O_2 binding affinity ($P_{50} \sim 7.5$ Torr) (*19*). However, this function is not yet excluded in the mammalian retina, where particularly high Ngb concentrations (~100 μM) have been reported (*20*). Other potential functions for Ngb include a role as a sensor for O_2 and NO levels (*21*), as a scavenger of reactive oxygen species, nitric oxide and other reactive nitrogen species (*19, 22, 23*), and/or as a guanine nucleotide dissociation inhibitor (*24*). Each hypothesis is supported by some evidence, but no clear-cut picture has yet emerged. It has been reported that expression of Ngb is upregulated under hypoxic and ischemic stress and has neuroprotective functions both in vitro and in vivo (*25*−*29*). However, the precise mechanism by which Ngb protects neurons against hypoxic or ischemic injury remains unclear.

In the presence of oxygen, the ferrous form of the pentacoordinated vertebrate globins, hemoglobin and myoglobin, is unstable and continuously undergoes a spontaneous oxidation (autoxidation), producing the ferric form and a superoxide radical (*30, 31*). Dismutation of the superoxide radical generates O_2 and H_2O_2. The latter is a potent two-electron oxidizing agent that can react further with both the ferrous and ferric forms of those globins to give a spectroscopically detectable ferryl (Fe^{IV}=O) species and, in the case of the ferric form, a transient protein radical (*32, 33*). The globin radical can be directly observed by EPR (*32, 33*), can be spin-trapped (*34, 35*), and, in the case of some hemoglobins and the myoglobin of sperm whales (*36, 37*), gives rise to dityrosine cross-linked oligomers. These studies have identified protein radicals on a variety of amino acid residues, primarily tyrosine (*34, 38, 39*), tryptophan (*40*), histidine (*38, 39*), and cysteine (*38, 39, 41*).

Spectroscopic studies with human and mouse recombinant Ngb show that the level of autoxidation of this type of protein is high compared with that of hemoglobin and myoglobin (*2, 19, 42*). However, the ferric form of Ngb does not react with the oxidizing agents H_2O_2 and peroxynitrite and, hence, does not produce the highly reactive ferryl species and a transient protein radical (*22*). The purpose of this investigation is to clarify the possible role(s) of the distal histidine residue, which provides the sixth coordination bond, in inhibiting these reactions.

EXPERIMENTAL PROCEDURES

Materials. Horse heart metmyoglobin (HoMb) acquired from USB (Cleveland, OH) was purified before use by being passed through a Sephadex G-25 gel filtration column (GE Healthcare Bio-Sciences, Piscataway, NJ) and elution with 50 mM potassium phosphate buffer (pH 6.8). HoMb concentrations were determined by measuring the absorbance of the heme Soret band using an $\varepsilon_{MetMb,408}$ of 188 mM^{-1} cm^{-1} (*43*). Trypsin (from bovine pancreas, modified, sequencing grade) and catalase from beef liver (suspension, 64000 units/mg) were obtained from Roche Molecular Biochemicals (Indianapolis, IN). Gelatin from cold water fish skin was obtained from Sigma (St. Louis, MO). DMPO (high purity, ≥99%) from Alexis Biochemicals (San Diego, CA) was sublimed twice under vacuum at room temperature and stored under an argon atmosphere at −70 °C before being used. The DMPO concentration was measured at 228 nm, assuming a molar extinction coefficient of 7800 M^{-1} cm^{-1} (*44*). All aqueous solutions were prepared using water passed through a Picopure 2UV Plus system (Hydro Services and Supplies, Inc., Research Triangle Park, NC) equipped with a 0.2 μm pore size filter. Diluted H_2O_2 solutions, obtained from a 30% solution (Fisher Scientific Co., Fairlawn, NJ), were used within 1 h of preparation. The H_2O_2 concentration was confirmed by absorbance measurements at 240 nm ($\varepsilon_{H_2O_2,240} = 39.4$ M^{-1} cm^{-1}) (*45*). All other chemicals were analytical grade and were purchased from Sigma or Roche Molecular Biochemicals. Absorption spectra were recorded on a Cary 100 UV−visible spectrometer (Varian, Victoria, Australia).

Preparation of Recombinant Proteins. The original construct of Ngb (cDNA of human Ngb in pET3a) was a generous gift from T. Laufs and T. Burmester. The full-length cDNA sequence of Ngb was subcloned into the *Nde*I and *Hin*dIII sites of vector pUC18 for prokaryotic expression. The two primers flanking the human neuroglobin gene were 5′-GGAATTCCATATGGAGCGCCCGGAGCCCGAGCTGATCCG-3′ (forward primer) and 5′-CCCAAGCTTTTACTCGCCATCCCAGC-3′ (reverse primer) with *Nde*I and *Hin*dIII restriction sites underlined. PCR was carried out with a GeneAmp 9700 DNA thermal cycler (Applied Biosystems, Foster City, CA) using PfuTurbo DNA polymerase (Stratagene, La Jolla, CA). The PCR was checked by agarose electrophoresis, and the amplified DNA fragment was purified with a QIAquick PCR purification kit (Qiagen Inc., Valencia, CA). The purified DNA fragment and pUC18 were digested separately with *Nde*I and *Hin*dIII and were ligated. The final plasmid was verified by DNA sequencing using BigDye terminator cycle sequencing and an ABI model 3100 sequencer (Applied Biosystems). The ligated plasmid was then used to transform *Escherichia coli* DH5α.

Cells were grown at 37 °C in Luria-Bertani medium containing 100 μg/mL ampicillin. After 18 h, the cells were harvested by centrifugation. All purification steps described below were performed at 4 °C. The cell pellets were resuspended in a 4-fold excess (with respect to the initial weight of cells) of lysis buffer [50 mM Tris-HCl buffer (pH 8.0) containing 1 mM EDTA, 1 mM dithiothreitol, 0.1 mM

phenylmethanesulfonyl fluoride, 4.5 μM leupeptin, 2.9 μM pepstatin, 3.3 μM antipain, 50 units of Dnase I/mL, 5 units of Rnase/mL, and 5% lysozyme]. The solution was stirred for 60 min, after which the cells were sonicated using a Branson (Danbury, CT) sonifier. Cell debris was removed by centrifugation and fractionated by ammonium sulfate precipitation (first 30% and then 45% saturation). The 45% ammonium sulfate pellet containing the crude Ngb was resuspended in a minimal volume of 10 mM Tris-HCl buffer (pH 7.5) (typically 1−2 pellet volumes) and dialyzed overnight against the same buffer. The crude dialyzed protein solution was then loaded onto a DEAE D52 anion exchange column (Whatman, Maidstone, U.K.), washed, and equilibrated in 10 mM Tris-HCl buffer (pH 7.5). After unbound material had been washed off, Ngb was eluted with 10 mM Tris-HCl buffer (pH 7.5) supplemented with 100 mM NaCl. The fractions containing the Ngb (as determined by absorbance at 400 nm) were pooled and concentrated by ultrafiltration using centricon YM-10 cartridges (Millipore Corp., Bedford, MA; molecular weight cutoff of 10000). The protein was then further purified on a Sephacryl S-200 HR column (2.5 cm × 67 cm) (GE Healthcare Bio-Sciences, Piscataway, NJ). The column was equilibrated, and separations were performed at a flow rate of 0.34 mL/min using 50 mM potassium phosphate buffer (pH 6.8). The fractions having the highest Ngb content ($A_{412}/A_{275} \geq 2.9$) were pooled and concentrated by ultrafiltration using centricon YM-10 cartridges. The purified protein was then stored at 4 °C in 50 mM potassium phosphate buffer (pH 6.8).

The expression of Ngb yields the protein in the $Fe^{2+}-O_2$ form. The met (Fe^{3+}) form (metNgb) was obtained by treating the protein with a 20% excess of $K_3Fe(CN)_6$ and quickly passing the resulting solution over a Sephadex G-25 gel filtration column equilibrated with 50 mM potassium phosphate buffer (pH 6.8). Samples were stored at −70 °C. Once thawed, the protein was kept on ice until it was used. Except when noted, in all the experiments described below, the proteins (wild-type Ngb and H64V variant protein) were utilized in their met form. MetNgb concentrations were estimated by measuring the absorbance of the heme Soret band using an ε_{414} of 129 mM^{-1} cm^{-1} (*46*).

Site-Directed Mutagenesis. A QuickChange site-directed mutagenesis system (Stratagene, La Jolla, CA) was used to replace the distal His-64 with Val-64 in human Ngb. The primers were 5′-CGCCTGAGTTTCTGGACGTGATCAG-GAAGGTGATGC-3′ (forward primer) and 5′-GCATCAC-CTTCCTGATCACGTCCAGAAACTCAGGCG-3′ (reverse primer) with the mutations underlined. The point mutation was confirmed by DNA sequencing. The recombinant mutant Ngb was subsequently expressed and purified as described above.

Oligomerization and SDS−PAGE of Protein Samples. Cross-linking experiments were performed by incubating solutions of either wild-type or H64V variant Ngb [protein concentration of 100 μM, each in 50 mM potassium phosphate (pH 6.8)] with 1 equiv of H_2O_2 at 25 °C. After 30 min, the reactions were terminated by addition of the SDS−PAGE sample buffer supplemented with 190 mM DTT [∼4 (v/v) protein solution:sample buffer, final concentration of 38 mM for DTT and 80 μM for Ngb]. Samples were allowed to stand in reducing sample buffer for 10 min and heated at 85 °C for 2 min before being loaded and separated onto 4 to 12% Bis-Tris NuPAGE (Invitrogen, Carlsbad, CA) gels, which were stained with Coomassie blue.

Fluorescence Detection of Dityrosine Cross-Links. Ngb solutions were prepared in potassium buffer and reacted with 1 equiv of H_2O_2 at 25 °C, as described above. After a 30 min incubation, the reaction mixtures were cooled to 4 °C and acidified to pH 2.5 by the addition of concentrated HCl. The heme was then extracted with 1 volume of cold 2-butanone. The organic layer containing the extracted heme was discarded. The aqueous solution containing the apoprotein was filtered using a Sephadex G-25 gel filtration column previously equilibrated and eluted with 200 mM sodium bicarbonate buffer (pH 9.4). The resulting mixtures were then diluted with the same buffer to a concentration of 2.1 μM. After 315 nm excitation, the fluorescence intensities of the resulting mixtures were measured over a range of wavelengths that bracket 410 nm, which is the emission maximum of the Tyr−Tyr bond, using a FluoroLog 3 spectrofluorimeter (Horiba Jobin Yvon, Edison, NY). All measurements were performed at 25 °C in a 5 mm × 5 mm supracil fluorescence cuvette. Dityrosine standard was synthesized and purified as described previously (*37*). The purity of the compound was checked by reverse phase HPLC and mass spectrometry.

Sample Preparation for Proteolytic Digestion. A 150 μM Ngb solution was prepared in 50 mM potassium phosphate buffer (pH 6.8) containing 50 μM DTPA. The reaction was conducted at 25 °C using 100 mM DMPO and was initiated by the addition of 3 equiv of H_2O_2. After a 30 s incubation, the excess H_2O_2 was removed by adding catalase (250 units/mL). The resulting solution was cooled to 4 °C, and the heme was then extracted with 1 volume of cold 2-butanone, as described above. The aqueous solution containing the apoprotein was filtered using a Sephadex G-25 gel filtration column previously equilibrated and eluted with 100 mM Tris-HCl (pH 8.5). The fraction having the highest Ngb content (∼50 μM) was digested using a 20:1 substrate:trypsin ratio for 16 h at 37 °C. Reactions were stopped by injecting the final mixture directly onto a reverse phase high-pressure liquid chromatography (RP-HPLC) column.

Fractionation of Protein Digest by RP-HPLC. All RP-HPLC experiments were performed on a Chemstation 1100 liquid chromatography system (Agilent Technologies, Palo Alto, CA), equipped with a control module, vacuum degasser, binary pump, manual injector, and diode-array UV-visible and fluorescence detectors. HPLC fractions were collected using a fraction collector (model 2110, Bio-Rad, Richmond, CA). Digested samples (50 μL) were injected onto a Vydac 218TP54, 4.6 mm × 250 mm, C18 RP-HPLC column (Vydac, Hesperia, CA). Peptides were eluted using a flow rate of 0.8 mL/min and a linear gradient from 100% solvent A to 50% solvent B over 80 min (solvent A, 0.1% trifluoroacetic acid in water; solvent B, 0.085% trifluoroacetic acid in acetonitrile). A rapid gradient to 90% solvent B and then back to 100% solvent A was used to regenerate the column. The eluent was monitored with a UV-visible detector set at 216 and 280 nm. Fractions (0.4 min) were collected in Eppendorf tubes containing 200 μL of 100 mM NH_4HCO_3 (pH 7.8). An aliquot of each fraction (50 μL) was analyzed via an ELISA; the rest of the fraction was lyophilized and stored at −70 °C for subsequent analyses.

ELISA. The rabbit anti-DMPO nitrone adduct polyclonal antiserum developed in this laboratory has already been

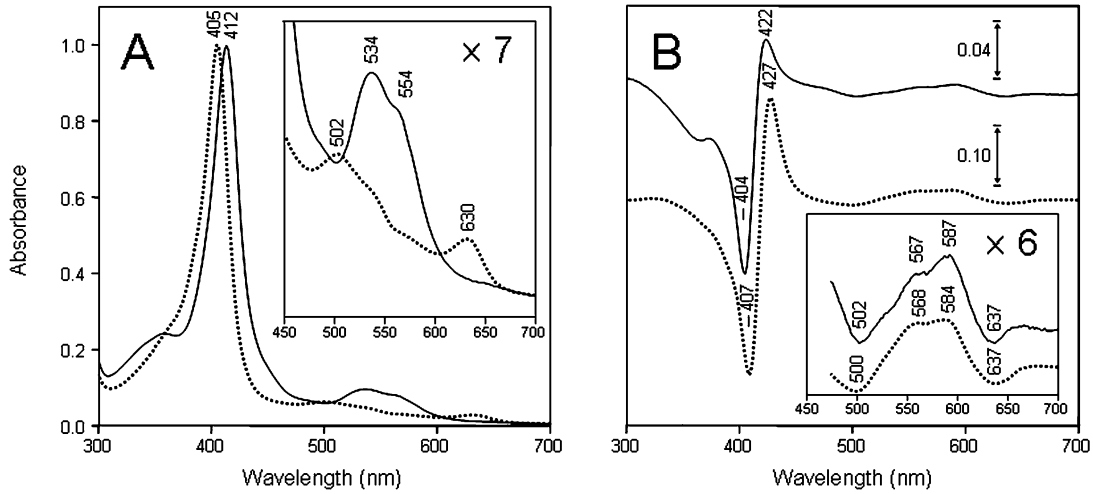

FIGURE 1: Absorption spectra of the wild type and H64V variant of human neuroglobin. (A) Wild-type human metNgb (—) and the metH64V variant (•••). The spectra were recorded directly after oxidation by ferricyanide. (B) Difference between spectra of the metH64V variant (—) and of commercial horse heart metmyoglobin (•••) recorded before and after the addition of 1 equiv of H_2O_2. Spectra in panel B were recorded before and within 6 s of addition of H_2O_2. The visible region of each spectrum (450−700 nm) has been enlarged at the magnification indicated on the right side of each figure. Experimental conditions: metNgb (7.8 μM) or metMb (5.3 μM) in 50 mM potassium phosphate buffer (pH 6.8) at 25 °C.

described (*47*). Protein-derived nitrone adducts were assessed using standard ELISAs in 96-well plates (Greiner Labortechnik, Frickenhausen, Germany). Reaction mixtures were first diluted with coating buffer [100 mM sodium bicarbonate (pH 9.6)] to a concentration of 0.2 μM, and 300 μL of this dilution was applied to each well (1.0 μg of protein per well). ELISA analyses were then performed as previously described (*39*). ELISA analyses of HPLC fractions were also performed as described previously (*39*).

Electrospray Mass Spectrometry. A Micromass Q-TOF Micro (Waters Micromass Corp., Manchester, U.K.) hybrid tandem mass spectrometer was used for the acquisition of the electrospray ionization (ESI) mass spectra and tandem mass spectra. All experiments were performed in the positive ion mode. HPLC fractions showing positive ELISA signals were resuspended in a minimal volume (~50 μL) of a 50:50 water/acetonitrile mixture containing 0.1% formic acid and infused into the mass spectrometer at ~300 nL/min using a pressure injection vessel. The needle voltage was ~3000 V, and the collision energy was 10 eV for the MS analyses. Collision-induced dissociation experiments employed argon as the collision gas with a collision energy between 30 and 50 eV. Data analysis was accomplished with a MassLynx data system and MaxEnt deconvolution software supplied by the manufacturer.

RESULTS

A key feature of Ngb is its six-coordinate heme structure in both the ferrous and ferric states, with the distal histidine (His-64) forming an endogenous ligand (*2, 5, 6*). To clarify the possible role(s) of the distal histidine residue in protecting the Fe(III) center of Ngb from attack by strong oxidants, a mutant of Ngb in which the distal histidine was replaced with valine, an oxidation-inert amino acid, was constructed and expressed. The mutant protein was purified by the same protocol as, and in yields comparable to, the wild-type protein. Purity was checked by SDS−PAGE and showed a single band at approximately 17 kDa (>95% pure, not shown).

Direct Observation of a Peroxidase-like Ferryl (Fe^{IV}=O) Species. Absorption spectra recorded directly after the purification of the wild-type Ngb and the H64V variant proteins were similar (data not shown) and showed the typical features of oxyferrous globins (*43*). The oxyferrous Ngbs were converted to their ferric forms (metNgb) by addition of ferricyanide. The spectrum obtained for wild-type Ngb after treatment with the oxidizing reagent [Figure 1A (—)] is typical for hexacoordinated ferric globins (λ_{max} at 412 and 534 nm and a shoulder around 554 nm) (*2*). When the H64V variant protein was treated in the same way [Figure 1A (•••)], the spectrum became similar to that of the ferric form of pentacoordinated globins (λ_{max} at 405, 502, and 630 nm) but differed markedly from that of the ferric form of wild-type Ngb; this is in accord with previous observations (*48*).

The formation of ferryl (Fe^{IV}=O) species in the reaction of wild-type human Ngb and H64V variant proteins with H_2O_2 was then investigated. In agreement with previous investigations (*22*), no changes were observed in the spectra of oxyferrous forms of either wild-type or H64V variant proteins or wild-type metNgb, even after addition of a large excess of the oxidant (up to 2 mM H_2O_2) (data not shown). However, small but significant changes can be observed in the spectrum of the metH64V mutant after the addition of 1 equiv of H_2O_2 [Figure 1B (—)]. The data are presented as the difference between spectra to better visualize the changes because changes were too weak to provide clear information in direct mode. The difference between spectra of horse metmyoglobin recorded before and after the addition of 1 equiv of H_2O_2 is shown in the same figure for comparison [Figure 1B (•••)].

Addition of H_2O_2 to the metH64V mutant resulted in a red shift in the Soret absorbance maximum (maximum variations in difference spectra at 404 and 422 nm) coupled with an increase in the visible range (maximum variations in difference spectra at 502, 567, 587, and 637 nm) [Figure 1B (solid line)]. These maxima correspond closely to those for horse metMb after the addition of H_2O_2 (maximum variations in difference spectra at 407, 427, 500, 568, 584,

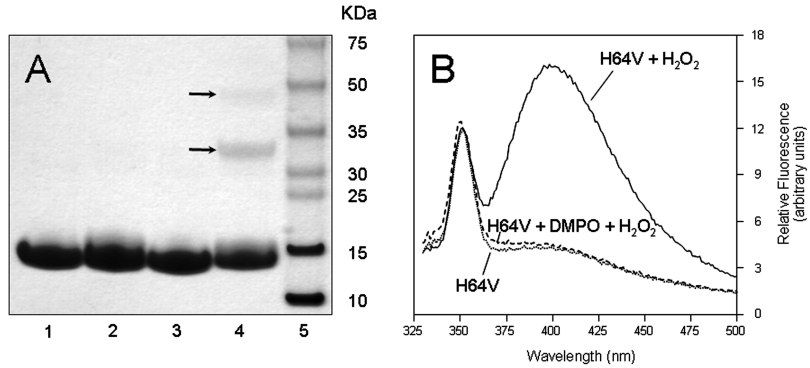

FIGURE 2: (A) SDS−PAGE analysis of human neuroglobin following H_2O_2 treatment: lane 1, wild-type metNgb; lane 2, wild-type metNgb and H_2O_2; lane 3, metH64V mutant; lane 4, metH64V mutant and H_2O_2; lane 5, molecular mass standards. Arrows indicate positions for dimeric and trimeric products. The samples were reduced with DTT and were boiled before electrophoresis. (B) Fluorescence emission spectra of the H64V mutant before and after addition of 1 equiv of H_2O_2: (•••) metH64V mutant, (—) metH64V mutant and H_2O_2, and (---) metH64V mutant, DMPO, and H_2O_2. The excitation wavelength was set at 315 nm. The emission spectra were measured over a range of wavelengths that bracket 410 nm, the emission maximum of the Tyr−Tyr bond. Incubations and heme extraction procedures were carried out as described in Experimental Procedures. The following concentrations were used: 100 μM Ngb and H_2O_2 (A and B) and 100 mM DMPO (B).

and 637 nm) [Figure 1B (•••)] and are typical for the conversion of a ferric heme to a ferryl species. The metH64V mutant ferryl species was stable for a few seconds up to 2 min, depending on the excess of H_2O_2 (data not shown). The addition of catalase within 30 s of the addition of H_2O_2 resulted in a quick reversion of a fraction of the ferryl to the native ferric form. However, differences between the original and final heights at 404 nm suggest a partial degradation of the prosthetic heme group during the process (not shown).

H_2O_2-Mediated Oligomerization of the H64V Mutant. In addition to its notable impact upon absorption spectra, the addition of H_2O_2 led to metNgb oligomerization. SDS−PAGE analysis of nontreated metNgb showed a single band at approximately 17 kDa corresponding to the neuroglobin monomer (Figure 2A, lane 1). However, analysis of metNgb after incubation with H_2O_2 showed that the monomeric H64V mutant was partially converted to dimeric and trimeric products (Figure 2A, lane 4, arrows) while the wild-type human metNgb was not (Figure 2A, lane 2). Formation of trimeric products suggests that at least two residues in separate locations on the Ngb surface can participate in oligomerization reactions. These cross-linking reactions cannot be attributed to S−S bond formation, as the protein samples were treated with DTT before electrophoresis.

Previous investigations have established that the reaction of some hemoproteins with H_2O_2 results in oligomerization of the protein due to the formation of tyrosine−tyrosine cross-links (*37*). The dityrosine cross-links can be detected by their characteristic ultraviolet fluorescence (*49*). This led us to compare the fluorescence spectrum of the H64V variant metNgb protein before and after incubation with H_2O_2. As one can see in Figure 2B (—), the H_2O_2-treated mutant protein exhibits an additional emission maximum around 410 nm when exposed to 315 nm light, consistent with formation of dityrosine cross-links (*49*). Dityrosine is a covalently bound diphenol, produced by the reaction of two tyrosyl radicals. Thus, the formation of a dityrosine cross-link between Ngb molecules provides the first solid evidence that a protein radical is indeed formed in the reaction of metNgb with H_2O_2. The low-intensity peak which occurs at 355 nm, the Raman band for water, is also observed in the two spectra. Interestingly, dityrosine fluorescence was not detected when the H64V variant metNgb protein was treated with H_2O_2 in the presence of the spin trap DMPO [Figure 2B (---)].

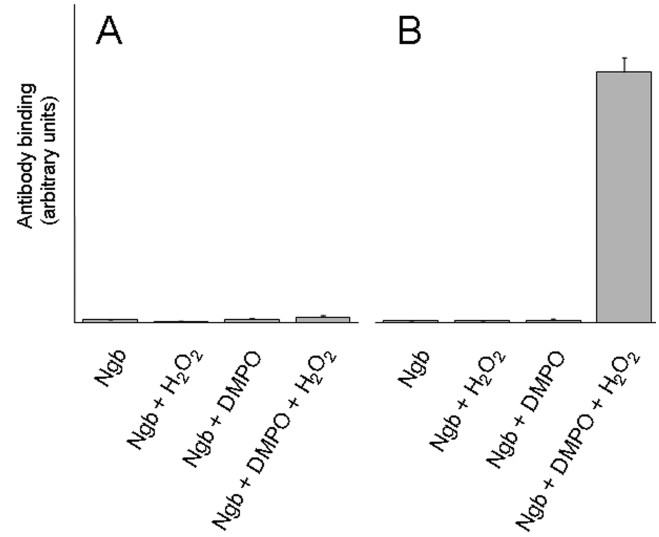

FIGURE 3: Immunochemical detection of wild-type and H64V recombinant human metNgb radical-derived nitrone adducts: (A) wild-type metNgb and (B) H64V metNgb. H_2O_2-dependent formation of globin radical-derived DMPO nitrone adduct was examined by ELISA analyses. Reaction mixtures containing globin in met form (1 μM), DMPO (100 mM), H_2O_2 (10 μM), or subsets of these as indicated were incubated in 50 mM potassium phosphate buffer (pH 6.8). The reactions were initiated by adding H_2O_2 to the mixture of globin and the spin trap. After incubation for 30 min at 37 °C, reactions were stopped by the addition of 250 units/mL catalase and mixtures were diluted with coating buffer for ELISA analysis. Values are means ± the standard deviation ($n = 3$).

Immunochemical Detection of Globin-Centered Radicals. Immuno-spin trapping (*47*) was used to confirm protein-derived radical formations in the reaction of metNgb with H_2O_2. Anti-DMPO antibody binding to the globin−DMPO adduct was assessed using an ELISA (Figure 3). When the H64V variant metNgb protein was treated with H_2O_2 in the presence of DMPO, nitrone adducts were detected (Figure 3B). In contrast, no adducts were detected when the wild-type metNgb protein was treated with H_2O_2 (Figure 3A) or in any of the control samples lacking DMPO or H_2O_2.

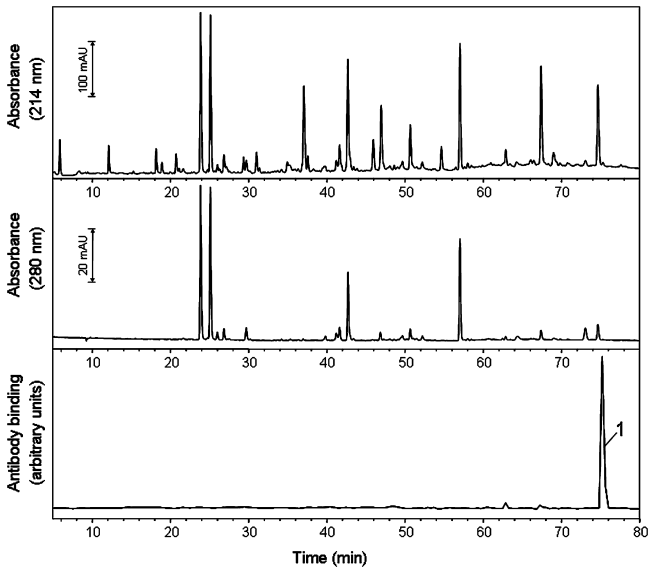

FIGURE 4: Reversed phase HPLC of the tryptic digest of the metNgb H64V mutant reacted with H_2O_2 in the presence of DMPO. Absorbances were monitored at 214 nm (peptide backbone) and 280 nm (aromatic amino acid). Fractions of 320 μL were collected every 0.4 min, and a 50 μL aliquot of each fraction was analyzed with an ELISA (bottom trace). Only one fraction exhibited strong anti-DMPO binding (peak 1) and was further characterized by tandem mass spectrometry.

Mass Spectrometry Assessment of Disulfide Bonds and of DMPO Trapping Yields. Analysis of wild-type Ngb and the H64V variant protein by flow injection electrospray ionization mass spectrometry indicated the presence of one free cysteine and one disulfide bond (data not shown); this result is in accord with previous observations obtained for the wild-type protein (*15*). When the H64V variant metNgb protein was analyzed by ESI, no ions corresponding to protein−DMPO adducts were observed after reaction with H_2O_2 in the presence of DMPO (data not shown). This result indicates that under the conditions used in this study the trapping yields are low.

MS Identification of the Amino Acid Residue Labeled with the Spin Trap. Identification of the specific location of the DMPO adduct on the H64V variant Ngb protein was determined by a mass spectrometry method that combines off-line immuno-spin trapping and chromatographic procedures (*39*). In this technique, the protein-DMPO nitrone adducts are proteolytically digested, peptides are separated by HPLC, and the collected fractions are analyzed with an ELISA using polyclonal anti-DMPO nitrone antiserum. Fractions showing positive ELISA signals are then concentrated and characterized by tandem mass spectrometry (MS/MS). This method adds a dimension of selectivity prior to the MS analysis, thereby facilitating the identification of the actual amino acid(s) labeled by the spin trap (*39*).

The HPLC chromatograms for the tryptic digest of the H64V variant metNgb protein treated with H_2O_2 in the presence of DMPO are shown in Figure 4 (top and middle panels). The bottom panel shows the results of ELISA analyses. Only one HPLC fraction exhibited a strong positive ELISA signal (peak 1), so this fraction was further characterized using flow injection analysis coupled to electrospray ionization mass spectrometry (ESI-MS) and tandem mass spectrometry (MS/MS). The ESI mass spectrum of the ELISA-positive fraction is shown in Figure 5. The ions at *m/z* 969.79 (+3) and *m/z* 1454.13 (+2) correspond in mass to tryptic peptide T8 (residue 70-96), which has a theoretical mass of 2906.5 Da [calculated mass-to-charge (*m/z*) values of 1454.26 (+2) and 969.84 (+3)]. The ions at *m/z* 1006.80 (+3) and *m/z* 1509.63 (+2) correspond in mass to the addition of one molecule of DMPO to tryptic peptide T8. The inset in Figure 5 depicts one pair of triply charged ions, which shows a mass-to-charge difference of 37.0. This mass difference corresponds to the loss of one molecule of DMPO (111.07, theoretical mass shift) and depends on the charge state; i.e., Δm = 111.07 (+1), 55.54 (+2), or 37.02 (+3). As demonstrated in our previous investigation (*39*), these pairs of ions can greatly facilitate the selection of DMPO-containing ions of interest and are characteristic of Tyr-DMPO modifications.

To determine the position of DMPO within this peptide, each pair of ions observed in Figure 5 was subjected to MS/MS analysis. An example of an MS/MS spectrum which allows for the sequence determination for the DMPO-containing triply charged pair of ions is presented in Figure 6. These data show a series of carboxy-terminal y ions (y_4, y_6, and y_8-y_{25}) and amino-terminal b ions (b_2-b_5, b_7, and b_8), accounting for most of the amino acids in the Val-68-Arg-94 sequence. The series y_8-y_{25} corresponds to a shift in mass of an additional 111 Da when compared to the same series in the MS/MS spectrum of the unmodified peptide. These data, together with normal y ions y_6 and y_4, allow the assignment of a DMPO molecule either to Glu-87 or to Tyr-88 of tryptic peptide T8 of the H64V variant of Ngb. Given that Glu-87 is an oxidation-inert amino acid, the data are most consistent with the formation of the DMPO nitrone adduct at Tyr-88.

DISCUSSION

In contrast to the ferric forms of myoglobin (metMb) and hemoglobin (metHb), the ferric form of Ngb (metNgb) does not produce a peroxidase-like ferryl (Fe^{IV}=O) species and a transient protein radical when treated with H_2O_2 (*22*). Also, in contrast to metMb and metHb, metNgb does not generate an Fe^{IV}=O species on reaction with $ONOO^-$ (peroxynitrite) (*22*). To clarify the possible role(s) of the distal histidine residue in inhibiting these reactions, a mutant of Ngb in which the distal histidine is replaced with valine, an oxidation-inert amino acid, was constructed and expressed. It is shown here that, in the presence of H_2O_2, the metH64V mutant produced DMPO-trappable protein radicals, as detected by immuno-spin trapping (Figure 3). This finding provides the first solid evidence that a protein radical is formed in the reaction of H_2O_2 with a variant of metNgb lacking a distal coordination bond with His-64. In contrast, no adducts were detected when the hexacoordinated wild-type metNgb was treated with H_2O_2, which confirms the critical role of the distal histidine residue in inhibiting this reaction.

The specific location(s) of the DMPO adduct(s) on H64V variant protein was determined by a mass spectrometry method that combines off-line immuno-spin trapping and chromatographic procedures. Only one HPLC fraction exhibited a strong positive ELISA signal (Figure 4); therefore, this fraction was further characterized by electrospray ionization mass spectrometry (ESI-MS) and MS/MS. An

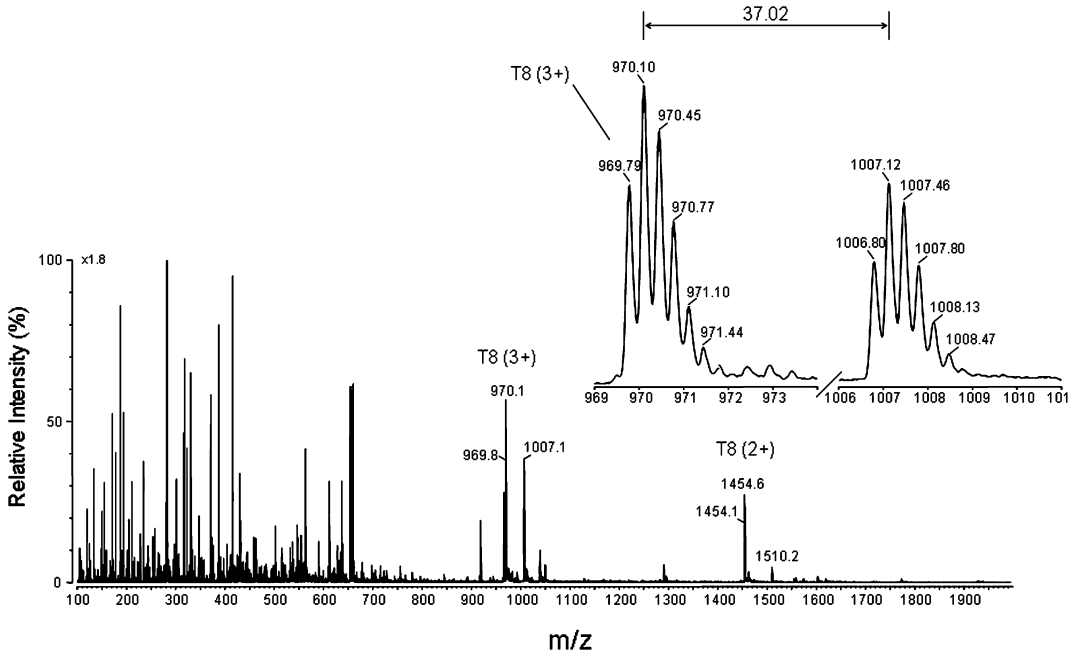

FIGURE 5: Full scan mass spectrum of the fraction that exhibited anti-DMPO binding. The fraction corresponding to peak 1 in Figure 4 and eluting at approximately 75.4 min was lyophilized, resuspended in a 50:50 acetonitrile/H_2O mixture with 0.1% formic acid, and directly infused into the electrospray source of a Micromass Q-TOF hybrid tandem mass spectrometer. An expanded view of a pair of ions having the same charge state (+3 ions) and a mass-to-charge (*m*/*z*) difference of 37.0 is shown. This mass difference corresponds to the loss of one molecule of DMPO.

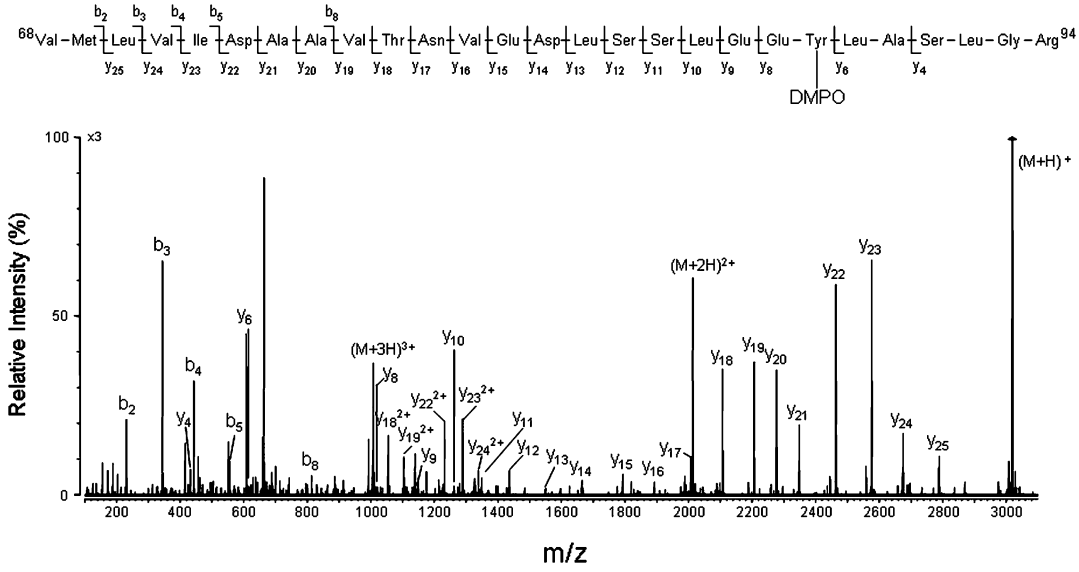

FIGURE 6: Deconvoluted MS/MS spectrum acquired from a parent ion of *m*/*z* 1006.8 (+3 ion), which corresponds in mass to tryptic peptide T8 plus DMPO. For the sake of clarity, not all identified fragment ions are labeled on the spectrum.

abundant ion that corresponds in mass to tryptic peptide T8 (amino acids residues 68−94) with a DMPO molecule was observed (Figure 5). MS/MS analysis by collision-induced dissociation revealed Tyr-88 to be the sole site of modification by DMPO on this peptide (Figure 6). No other DMPO-modified tryptic peptide was detected.

There are four tyrosine residues in human Ngb (i.e., Tyr-44, Tyr-88, Tyr-115, and Tyr-137). From the crystal structure of human Ngb in its hexacoordinated ferric form, determined at 1.95 Å resolution (*5*), three of the tyrosyl residues exhibit at least some degree of solvent accessibility (i.e., Tyr-44, Tyr-88, and Tyr-115) while Tyr-137 is an internal residue. Tyr-88, the only tyrosine residue detectably modified by DMPO, is the tyrosine residue nearest the heme group, and the shortest distance separating these two groups is 3.85 Å (Figure 7). This distance is similar to the corresponding distance in both the unliganded ferric (*6*) and CO-bound ferrous (*14*) forms of murine Ngb. In the human variant protein, the phenol oxygen of Tyr-88 actually points toward a large cavity [$\sim$120 Å^3 for human Ngb, (*5*)], which stretches from the heme distal site toward the protein surface. Tyr-88 is thus optimally placed for oxidation by reactive species generated on the porphyrin ring structure and for the production of DMPO-trappable tyrosyl radicals.

The finding that the H64V Ngb mutant undergoes a dimerization reaction in which a tyrosine residue in each of two Ngb molecules couples to give a dityrosine cross-link provides additional evidence of a protein radical and confirms

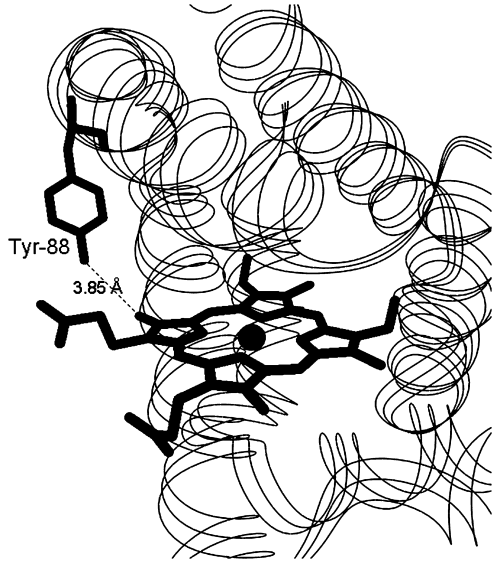

FIGURE 7: Location of the radical-forming tyrosyl residue identified in this study and its position relative to the heme prosthetic group. The atomic coordinates were obtained from ref *5* and the Protein Data Bank (entry 1OJ6). Tyr-88 is the tyrosine residue nearest the prosthetic heme group. The point of closest approach is the phenol oxygen, which is located 3.85 Å from the carbon atom of one of the heme methyl groups.

that the radical generated on the globin is partly localized on a tyrosine residue. The nature of the cross-link was definitively established by fluorescence spectrometry [Figure 2B (—)], but the identity of the two cross-linked residues remains to be determined. One possibility is that the reaction of the H64V mutant with H_2O_2 yields dimers linked by Tyr-88−Tyr-88 cross-links. The finding that preincubation of Ngb with DMPO prevents dityrosine formation [Figure 2B (---)] may indicate that formation of a nitrone adduct at position Tyr-88 suppresses subsequent cross-linking of this residue. It is also possible that the protection by 100 mM DMPO against dimerization is due to reducing impurities in the spin trap. However, the observation that in the absence of DMPO the monomeric H64V variant protein was partially converted, not only to dimeric but also to trimeric products, implicates at least one residue in addition to Tyr-88 as a locus of unpaired electron density. Note that the dimeric and trimeric products were not observed when the hexacoordinated wild-type metNgb was treated with H_2O_2, again showing the critical role of the distal histidine ligand in inhibiting this reaction.

This study indicates that a ferryl species is formed in parallel with formation of the protein radicals in the reaction of the metH64V variant protein with H_2O_2 (Figure 1B). Mb and Hb have long been known to form ferryl species upon treatment of the ferric state with peroxide (*32, 33*). In the reaction of the ferric form of Ngb with H_2O_2, however, a ferryl species has never been reported. Previous stopped-flow UV-vis rapid-scan experiments (*50*) suggest that the reaction of metMb may first produce a transient Compound I-like intermediate in which the ferryl species is coupled to a porphyrin rather than a protein radical. Electron transfer from the protein to the porphyrin radical cation would then produce the observed protein radical.

Although the reaction of metNgb with H_2O_2 has not yet been investigated by stopped-flow methods, it is likely that the H64V variant metNgb, lacking a distal coordination bond with His-64, acts as a pentacoordinated metMb and, thus, that a Compound I-like intermediate with a porphyrin-centered radical is also formed in this reaction. Compound I may subsequently channel the oxidizing equivalent located on the porphyrin ring to Tyr-88 and also, possibly via additional intra- and/or intermolecular electron transfer reactions, toward additional tyrosine residues. Some of the resulting Tyr−phenoxyl radicals may further react in a bimolecular reaction to generate the dityrosine cross-links detected in this study, while the Tyr-88−phenoxyl radical can be spin trapped by DMPO.

In summary, the replacement of a distal histidine (His-64) with a nonoxidizable amino acid enabled us to observe a ferryl species and a transient protein radical in the reaction of metNgb with H_2O_2. More specifically, Tyr-88 was identified as a site of tyrosyl radical formation in the peroxide-treated H64V variant metNgb, as detected with the spin trap agent DMPO. The presence of His-64 in the wild-type protein results in a complete loss of any detectable radical adduct and of the ferryl species. Together, the data reinforce the contention that wild-type Ngb is protected from attack by H_2O_2 and other strong oxidants by the coordinated distal His. In addition, this work further illustrates the power of the newly developed immuno-spin trapping approach in conjunction with chromatographic and mass spectrometric procedures in selecting DMPO-labeled peptides and identifying sites of DMPO covalent attachments, an attachment which occurs only subsequent to DMPO trapping of free radicals.

ACKNOWLEDGMENT

We thank Dr. Arno Siraki and Dr. Marilyn Ehrenshaft for their careful review of the manuscript and Ms. Jean Corbett, Ms. Anne Froment, Mrs. Mary J. Mason, and Dr. Ann Motten for their valuable assistance in the preparation of the manuscript. We thank Dr. Robert Petrovich and all the members of the Protein Expression Core Facility for their kind access to PCR machines and shakers and for their comments and suggestions. We are also grateful to Piotr Bilski for performing the fluorescence measurements. The original construct of Ngb in pET3a was a generous gift from Dr. Tilmann Laufs and Prof. Thorsten Burmester from the Institute of Zoology of the University of Mainz (Mainz, Germany).

REFERENCES

1. Burmester, T., Weich, B., Reinhardt, S., and Hankeln, T. (2000) A vertebrate globin expressed in the brain. *Nature 407*, 520–523.
2. Dewilde, S., Kiger, L., Burmester, T., Hankeln, T., Baudin-Creuza, V., Aerts, T., Marden, M. C., Caubergs, R., and Moens, L. (2001) Biochemical characterization and ligand binding properties of neuroglobin, a novel member of the globin family. *J. Biol. Chem. 276*, 38949–38955.
3. Van Doorslaer, S., Dewilde, S., Kiger, L., Nistor, S. V., Goovaerts, E., Marden, M. C., and Moens, L. (2003) Nitric oxide binding properties of neuroglobin. A characterization by EPR and flash photolysis. *J. Biol. Chem. 278*, 4919–4925.
4. Pesce, A., Bolognesi, M., Bocedi, A., Ascenzi, P., Dewilde, S., Moens, L., Hankeln, T., and Burmester, T. (2002) Neuroglobin and cytoglobin. Fresh blood for the vertebrate globin family. *EMBO Rep. 3*, 1146–1151.
5. Pesce, A., Dewilde, S., Nardini, M., Moens, L., Ascenzi, P., Hankeln, T., Burmester, T., and Bolognesi, M. (2003) Human brain neuroglobin structure reveals a distinct mode of controlling oxygen affinity. *Structure 11*, 1087–1095.
6. Vallone, B., Nienhaus, K., Brunori, M., and Nienhaus, G. U. (2004) The structure of murine neuroglobin: novel pathways for ligand migration and binding. *Proteins 56*, 85–92.

7. Mammen, P. P., Shelton, J. M., Goetsch, S. C., Williams, S. C., Richardson, J. A., Garry, M. G., and Garry, D. J. (2002) Neuroglobin, a novel member of the globin family, is expressed in focal regions of the brain. *J. Histochem. Cytochem. 50*, 1591–1598.
8. Awenius, C., Hankeln, T., and Burmester, T. (2001) Neuroglobins from the zebrafish *Danio rerio* and the pufferfish *Tetraodon nigroviridis*. *Biochem. Biophys. Res. Commun. 287*, 418–421.
9. Zhang, C., Wang, C., Deng, M., Li, L., Wang, H., Fan, M., Xu, W., Meng, F., Qian, L., and He, F. (2002) Full-length cDNA cloning of human neuroglobin and tissue expression of rat neuroglobin. *Biochem. Biophys. Res. Commun. 290*, 1411–1419.
10. Reuss, S., Saaler-Reinhardt, S., Weich, B., Wystub, S., Reuss, M. H., Burmester, T., and Hankeln, T. (2002) Expression analysis of neuroglobin mRNA in rodent tissues. *Neuroscience 115*, 645–656.
11. Kugelstadt, D., Haberkamp, M., Hankeln, T., and Burmester, T. (2004) Neuroglobin, cytoglobin, and a novel, eye-specific globin from chicken. *Biochem. Biophys. Res. Commun. 325*, 719–725.
12. Hankeln, T., Wystub, S., Laufs, T., Schmidt, M., Gerlach, F., Saaler-Reinhardt, S., Reuss, S., and Burmester, T. (2004) The cellular and subcellular localization of neuroglobin and cytoglobin; A clue to their function? *IUBMB Life 56*, 671–679.
13. Kriegl, J. M., Bhattacharyya, A. J., Nienhaus, K., Deng, P., Minkow, O., and Nienhaus, G. U. (2002) Ligand binding and protein dynamics in neuroglobin. *Proc. Natl. Acad. Sci. U.S.A. 99*, 7992–7997.
14. Vallone, B., Nienhaus, K., Matthes, A., Brunori, M., and Nienhaus, G. U. (2004) The structure of carbonmonoxy neuroglobin reveals a heme-sliding mechanism for control of ligand affinity. *Proc. Natl. Acad. Sci. U.S.A. 101*, 17351–17356.
15. Hamdane, D., Kiger, L., Dewilde, S., Green, B. N., Pesce, A., Uzan, J., Burmester, T., Hankeln, T., Bolognesi, M., Moens, L., and Marden, M. C. (2003) The redox state of the cell regulates the ligand binding affinity of human neuroglobin and cytoglobin. *J. Biol. Chem. 278*, 51713–51721.
16. Vinck, E., Van Doorslaer, S., Dewilde, S., and Moens, L. (2004) Structural change of the heme pocket due to disulfide bridge formation is significantly larger for neuroglobin than for cytoglobin. *J. Am. Chem. Soc. 126*, 4516–4517.
17. Brunori, M. (1999) Hemoglobin is an honorary enzyme. *Trends Biochem. Sci. 24*, 158–161.
18. Brunori, M. (2001) Nitric oxide moves myoglobin centre stage. *Trends Biochem. Sci. 26*, 209–210.
19. Fago, A., Hundahl, C., Dewilde, S., Gilany, K., Moens, L., and Weber, R. E. (2004) Allosteric regulation and temperature dependence of oxygen binding in human neuroglobin and cytoglobin. Molecular mechanisms and physiological significance. *J. Biol. Chem. 279*, 44417–44426.
20. Schmidt, M., Giessl, A., Laufs, T., Hankeln, T., Wolfrum, U., and Burmester, T. (2003) How does the eye breathe? Evidence for neuroglobin-mediated oxygen supply in the mammalian retina. *J. Biol. Chem. 278*, 1932–1935.
21. Brunori, M., Giuffre, A., Nienhaus, K., Nienhaus, G. U., Scandurra, F. M., and Vallone, B. (2005) Neuroglobin, nitric oxide, and oxygen: Functional pathways and conformational changes. *Proc. Natl. Acad. Sci. U.S.A. 102*, 8483–8488.
22. Herold, S., Fago, A., Weber, R. E., Dewilde, S., and Moens, L. (2004) Reactivity studies of the Fe(III) and Fe(II)NO forms of human neuroglobin reveal a potential role against oxidative stress. *J. Biol. Chem. 279*, 22841–22847.
23. Fordel, E., Thijs, L., Moens, L., and Dewilde, S. (2007) Neuroglobin and cytoglobin expression in mice. Evidence for a correlation with reactive oxygen species scavenging. *FEBS J. 274*, 1312–1317.
24. Wakasugi, K., Nakano, T., and Morishima, I. (2003) Oxidized human neuroglobin acts as a heterotrimeric Gα protein guanine nucleotide dissociation inhibitor. *J. Biol. Chem. 278*, 36505–36512.
25. Sun, Y., Jin, K., Mao, X. O., Zhu, Y., and Greenberg, D. A. (2001) Neuroglobin is up-regulated by and protects neurons from hypoxic-ischemic injury. *Proc. Natl. Acad. Sci. U.S.A. 98*, 15306–15311.
26. Sun, Y., Jin, K., Peel, A., Mao, X. O., Xie, L., and Greenberg, D. A. (2003) Neuroglobin protects the brain from experimental stroke in vivo. *Proc. Natl. Acad. Sci. U.S.A. 100*, 3497–3500.
27. Li, R. C., Lee, S. K., Pouranfar, F., Brittian, K. R., Clair, H. B., Row, B. W., Wang, Y., and Gozal, D. (2006) Hypoxia differentially regulates the expression of neuroglobin and cytoglobin in rat brain. *Brain Res. 1096*, 173–179.
28. Shang, A., Zhou, D., Wang, L., Gao, Y., Fan, M., Wang, X., Zhou, R., and Zhang, C. (2006) Increased neuroglobin levels in the cerebral cortex and serum after ischemia-reperfusion insults. *Brain Res. 1078*, 219–226.
29. Khan, A. A., Wang, Y., Sun, Y., Mao, X. O., Xie, L., Miles, E., Graboski, J., Chen, S., Ellerby, L. M., Jin, K., and Greenberg, D. A. (2006) Neuroglobin-overexpressing transgenic mice are resistant to cerebral and myocardial ischemia. *Proc. Natl. Acad. Sci. U.S.A. 103*, 17944–17948.
30. Rifkind, J. M., Ramasamy, S., Manoharan, P. T., Nagababu, E., and Mohanty, J. G. (2004) Redox reactions of hemoglobin. *Antioxid. Redox Signaling 6*, 657–666.
31. Tajima, G., and Shikama, K. (1987) Autoxidation of oxymyoglobin. An overall stoichiometry including subsequent side reactions. *J. Biol. Chem. 262*, 12603–12606.
32. Keilin, D., and Hartree, E. F. (1950) Reaction of methaemoglobin with hydrogen peroxide. *Nature 166*, 513–514.
33. King, N. K., and Winfield, M. E. (1963) The mechanism of metmyoglobin oxidation. *J. Biol. Chem. 238*, 1520–1528.
34. Gunther, M. R., Tschirret-Guth, R. A., Witkowska, H. E., Fann, Y. C., Barr, D. P., Ortiz De Montellano, P. R., and Mason, R. P. (1998) Site-specific spin trapping of tyrosine radicals in the oxidation of metmyoglobin by hydrogen peroxide. *Biochem. J. 330*, 1293–1299.
35. Davies, M. J. (1990) Detection of myoglobin-derived radicals on reaction of metmyoglobin with hydrogen peroxide and other peroxidic compounds. *Free Radical Res. Commun. 10*, 361–370.
36. Giulivi, C., and Davies, K. J. (1993) Dityrosine and tyrosine oxidation products are endogenous markers for the selective proteolysis of oxidatively modified red blood cell hemoglobin by (the 19 S) proteasome. *J. Biol. Chem. 268*, 8752–8759.
37. Lardinois, O. M., and Ortiz de Montellano, P. R. (2003) Intra- and intermolecular transfers of protein radicals in the reactions of sperm whale myoglobin with hydrogen peroxide. *J. Biol. Chem. 278*, 36214–36226.
38. Deterding, L. J., Ramirez, D. C., Dubin, J. R., Mason, R. P., and Tomer, K. B. (2004) Identification of free radicals on hemoglobin from its self-peroxidation using mass spectrometry and immuno-spin trapping: Observation of a histidinyl radical. *J. Biol. Chem. 279*, 11600–11607.
39. Lardinois, O. M., Detweiler, C. D., Tomer, K. B., Mason, R. P., and Deterding, L. J. (2008) Identifying the site of spin trapping in proteins by a combination of liquid chromatography, ELISA, and off-line tandem mass spectrometry. *Free Radical Biol. Med. 44*, 893–906.
40. DeGray, J. A., Gunther, M. R., Tschirret-Guth, R., Ortiz de Montellano, P. R., and Mason, R. P. (1997) Peroxidation of a specific tryptophan of metmyoglobin by hydrogen peroxide. *J. Biol. Chem. 272*, 2359–2362.
41. Witting, P. K., Douglas, D. J., and Mauk, A. G. (2000) Reaction of human myoglobin and H_2O_2. Involvement of a thiyl radical produced at cysteine 110. *J. Biol. Chem. 275*, 20391–20398.
42. Trent, J. T., 3rd, Watts, R. A., and Hargrove, M. S. (2001) Human neuroglobin, a hexacoordinate hemoglobin that reversibly binds oxygen. *J. Biol. Chem. 276*, 30106–30110.
43. Antonini, E., and Brunori, M. (1971) *Hemoglobin and Myoglobin in the Reactions with Ligands*, Elsevier, Amsterdam.
44. Buettner, G. R. (1990) On the reaction of superoxide with DMPO/$^{\bullet}$OOH. *Free Radical Res. Commun. 10*, 11–15.
45. Nelson, D. P., and Kiesow, L. A. (1972) Enthalpy of decomposition of hydrogen peroxide by catalase at 25 °C (with molar extinction coefficients of H_2O_2 solutions in the UV). *Anal. Biochem. 49*, 474–478.
46. Nicolis, S., Monzani, E., Ciaccio, C., Ascenzi, P., Moens, L., and Casella, L. (2007) Reactivity and endogenous modification by nitrite and hydrogen peroxide: does human neuroglobin act only as a scavenger? *Biochem. J. 407*, 89–99.
47. Mason, R. P. (2004) Using anti-5,5-dimethyl-1-pyrroline N-oxide (anti-DMPO) to detect protein radicals in time and space with immuno-spin trapping. *Free Radical Biol. Med. 36*, 1214–1223.
48. Uno, T., Ryu, D., Tsutsumi, H., Tomisugi, Y., Ishikawa, Y., Wilkinson, A. J., Sato, H., and Hayashi, T. (2004) Residues in the distal heme pocket of neuroglobin. Implications for the multiple ligand binding steps. *J. Biol. Chem. 279*, 5886–5893.
49. Malencik, D. A., and Anderson, S. R. (2003) Dityrosine as a product of oxidative stress and fluorescent probe. *Amino Acids 25*, 233–247.
50. Egawa, T., Shimada, H., and Ishimura, Y. (2000) Formation of compound I in the reaction of native myoglobins with hydrogen peroxide. *J. Biol. Chem. 275*, 34858–34866.

BI800771K